Vol. 594: 51–63, 2018
https://doi.org/10.3354/meps12559

MARINE ECOLOGY PROGRESS SERIES
Mar Ecol Prog Ser

Published April 26

Assessing phytoplankton community composition using combined pigment and particle size distribution analysis

Joan S. Font-Muñoz[1,*], Antoni Jordi[2,5], Sílvia Anglès[1], Pere Ferriol[3], Esther Garcés[4], Gotzon Basterretxea[1]

[1]Institut Mediterrani d'Estudis Avançats, IMEDEA (UIB-CSIC), Miquel Marqués 21, 07190 Esporles, Illes Balears, Spain
[2]Davidson Laboratory, Stevens Institute of Technology, Hoboken, NJ 07030, USA
[3]Universitat de les Illes Balears, Cra. de Valldemossa, km 7.5, 07122 Palma, Illes Balears, Spain
[4]Departament de Biologia Marina i Oceanografia, Institut de Ciències del Mar (ICM), Consejo Superior de Investigaciones Científicas (CSIC), 08003 Barcelona, Spain

[5]*Present address:* Jupiter Intelligence, Hoboken, NJ 07030, USA

ABSTRACT: Changes in phytoplankton composition reveal relevant information about the response of aquatic systems to environmental drivers. Here, we propose the combined use of particle size measurements and pigment signatures to analyze the changes in the composition of phytoplankton communities at a coastal location. Canonical correlation analysis (CCA) was applied to separate phytoplankton signals from non-algal components of particulate matter in concurrent measurements of particle size distribution and pigment concentrations (chlorophylls *a*, *b* and *c*). Using this method, we were able to identify phytoplankton community structure variations at size and functional levels associated with the water column during the spring to summer transition at a Mediterranean coastal site. Some taxa with characteristic size spectrum signatures such as *Pseudo-nitzschia* sp., which produced an intense (up to 5×10^5 cells l^{-1}), but ephemeral bloom, could also be identified. The general patterns of phytoplankton succession obtained using this methodology were corroborated by light microscopy and flow cytometry identification. Phytoplankton biovolume comparisons between both methods were highly consistent ($r = 0.75$, $p < 0.01$). We consider that combined pigment and size structure analysis using CCA is a useful tool to determine reorganization patterns of phytoplankton via changes in species composition.

KEY WORDS: Phytoplankton · Size distribution · Pigments · Canonical correlation analysis · Chlorophyll

INTRODUCTION

Phytoplankton communities are the foundation of ocean life, providing the energy that supports nearly all marine species and affecting biogeochemical cycling of carbon (Falkowski & Raven 2013). They are also highly responsive to changes in environmental conditions; therefore, variations in phytoplankton composition play a crucial role in structuring marine food webs, and are also accurate indicators of ecosystem-level perturbations (Margalef 1963, Irwin et al. 2006, Harris 2012, Guinder & Molinero 2013). Indeed, the study of the links between environmental conditions and phytoplankton community composition, and the analysis of the changes in community structure in response to key ecosystem and biogeochemical processes, such as primary production, carbon export and nitrogen fixation, are major objectives of current biological oceanography (Karl et al. 2001, Boyd et al. 2010).

Variations in size structure and community composition determined from pigment analysis reveal rele-

*Corresponding author: jfont@imedea.uib-csic.es

vant information on the shifts in the functioning of marine ecosystems in response to different environmental forcings (e.g. Lohrenz et al. 2003). Changes in pigments and size spectra can be indicative of variations in the way matter is processed throughout the food web, seasonal succession and multitrophic-level effects in phytoplankton communities. For example, changes in size structure from dominance of small picoplankton to larger nano- and microphytoplankton are associated with a variation from rapid carbon cycling by the microbial loop to dominance of more lineal food chains and increases in the biological pump due to more rapid sedimentation of particulate matter (Azam et al. 1983, Laws et al. 2000).

For a long time, conventional light microscopy has been the main tool for the identification and quantification of phytoplankton. However, because of the large number of species present in aquatic systems, detailed descriptions of phytoplankton assemblages at the species level are time consuming. Also, large differences can emerge from the different ways of analyzing the samples depending on the number of cells counted, the size of the sample examined and differences in the identification and counting criteria used by the taxonomists (Jakobsen et al. 2015, Zingone et al. 2015). Finally, microscopy analysis has limitations, particularly for the differentiation of small-sized species that dominate the phytoplankton community in many areas (Goericke 2011). These constraints of morphological cell identification have stimulated scientific interest in alternative methods for phytoplankton assemblage characterization such as pigment analysis (Gieskes & Kraay 1983, Yentsch & Phinney 1985, Wright et al. 2005), variations in size structure (Marañón 2009, Huete-Ortega et al. 2010) and, more recently, molecular methods (Bornet et al. 2004, Rusch et al. 2010).

The characteristic signatures of pigments for the identification of phytoplankton groups have been summarized in various studies, but taxonomic identification from pigment signatures is not yet a straightforward task (Jeffrey & Hallegraeff 1987, Gieskes 1991, Millie et al. 1993). The analysis of pigments obtained from either field samples or remotely sensed radiances is a widely used technique for the characterization of phytoplankton assemblages (Beutler et al. 2002). For example, spectrofluorometrically derived pigments, a readily available and affordable technique (Neveux et al. 2011), or more detailed HPLC pigment analyses and multivariate statistical analysis (i.e. CHEMTAX; Mackey et al. 1996), are routinely used for phytoplankton assessment to avoid laborious microscopy identification (Neveux & Lantoine 1993, Mackey et al. 1996, Uitz et al. 2006, Ras et al. 2008, Zhang et al. 2011). Nevertheless, pigment-based techniques can be limited when differentiating between groups sharing similar pigment markers, and hence information of community structure provided by pigment-based characterization may be incomplete.

Alternatively, phytoplankton can be assessed by their cell size. Size structure is an interesting characteristic because it is linked to key biological functions such as metabolism, productivity, growth and predation (Marquet et al. 2005, Litchman & Klausmeier 2008, Marañón 2015). Techniques such as image analysis and laser diffraction techniques (e.g. flow cytometers) are increasingly used for phytoplankton identification and size structure analysis (Haraguchi et al. 2017). Several sophisticated instruments have been developed to analyze phytoplankton communities *in situ*. Examples are the Imaging FlowCytobot (Olson & Sosik 2007), the CytoSense and the FlowCAM (Sieracki et al. 1998) that combine flow cytometry and image analysis to provide *in situ* measurements of the phytoplankton community at the genus or species level. While the future of plankton research increasingly relies on the use of these or similar instruments (Campbell et al. 2013, Dugenne et al. 2014, Thyssen et al. 2015), these new technologies for detection of phytoplankton at the group and species levels require careful training of the classification system (Sosik & Olson 2007, Anglès et al. 2015).

In the present study, we propose and test a simple and robust method to distinguish changes in the phytoplankton community using combined pigment and size structure information. Data obtained from fluorescence spectra and high-resolution *in situ* particle size distribution are analyzed using canonical correlation analysis (CCA) of the pigment–size relationships to infer changes in phytoplankton groups. Results from this method are validated with phytoplankton assemblage characterization by traditional microscopy and flow cytometry.

MATERIALS AND METHODS

Field sampling

To test the proposed methodology, a field study was carried out at a station located at a depth of 40 m (39.4894° N, 2.6744° E) in the inner part of Palma Bay, Mallorca (Fig. S1 in the Supplement at

www.int-res.com/articles/suppl/m594p051_supp.pdf). Twelve samplings were performed between 10 April and 26 September 2014 (see Table S1 in the Supplement for exact dates). During each sampling, continuous profiles of temperature, salinity and particle size distribution were obtained with an SBE-25 CTD and an attached laser *in situ* scattering and transmissometry (LISST)-100X transmissometer (Sequoia Scientific), respectively. Also, water samples for pigment analysis, phytoplankton identification and nutrient analysis were collected at 5 depths (5, 10, 20, 30 and 40 m) throughout the water column with a 2.5 l Niskin bottle.

Suspended particle size distribution, including both phytoplankton and other non-algal components, was measured using the LISST-100X. This instrument measures the particle size distribution as the particle volume concentration by size ranges (i.e. volume of particles in the seawater per unit volume of seawater) using a technique based on laser diffraction theory. The LISST uses a 670 nm collimated laser beam to illuminate the suspended particles, and a 32-ring detector measures the intensity of the scattered light, corresponding to 32 different size classes logarithmically spaced from 2.5 to 500 µm (Agrawal & Pottsmith 2000, Agrawal et al. 2008). The LISST was lowered vertically, attached to the CTD cage, with the sensor looking down to avoid direct sunlight, which can affect the measurements in the smallest size classes (Reynolds et al. 2010).

From each water sample, a 2 l subsample was filtered onto Whatman GF/F filters for spectrofluorometric pigment analysis and stored frozen until analysis in the lab. The filters were introduced in a centrifuge tube containing 10 ml of 90% acetone, and left in the dark at 4°C for a 24 h extraction. The tubes were then centrifuged for 5 min at 3500 rpm (2205 × *g*), and the spectral fluorescence matrices for excitation (400–480 nm) and emission (600–700 nm) were obtained with a Varian spectrofluorometer (Cary Eclipse model). Concentrations of chlorophylls (chl) *a*, *b* and *c* were estimated as in Neveux & Panouse (1987). Errors of this method with respect to the spectrophotometric measurements are 3–12% for chl *a*, 7–10% for chl *b* and 10–16% for chl *c*. The ratio between chl *b* and chl *c* is used as a taxon (or group) indicator. Higher values of chl *b* indicate the presence of *Prochlorococcus*, picoeukaryotes and nanoflagellates, while higher values of chl *c* are indicative of diatoms and dinoflagellates (Gibb et al. 2000). Light attenuation coefficients in the bay are generally low (0.06 ± 0.01 m^{-1} ± SD; authors' unpubl. data) and between 10 and 20% of surface irradiance penetrates to the vegetated sea floor at the sampling station. Therefore, it is unlikely that light affected our pigment measurements.

Another subsample of 150 ml was used for identification and quantification of nano- and microphytoplankton by means of light microscopy. The 150 ml samples were preserved with Lugol's iodine solution (1%). The general procedure for identifying and quantifying phytoplankton involved sedimentation (24 h) of a subsample in a 50 ml settling chamber, and subsequent counting of cells in an appropriate area (Throndsen 1995) using a Leica-Leitz DM-IRB inverted microscope.

Picoplankton was quantified by flow cytometry. A subsample of 2 ml was fixed in the dark for 30 min with paraformaldehyde plus glutaraldehyde (1 and 0.05% final concentrations, respectively), immediately stored in liquid nitrogen, and transferred to a –80°C freezer after arrival at the laboratory. The samples were analyzed with standard protocols on a Becton-Dickinson FACScalibur flow cytometer following the recommendations of Gasol & del Giorgio (2000).

Pico-, nano- and microphytoplankton cell concentrations were converted to biovolume estimates to compare with the LISST data. A disadvantage of the LISST is that the number of cells or particles from the particle size distribution can only be calculated assuming a spherical shape (Reynolds et al. 2010). This approximation may be valid for small coccoid cells or in cases of massive blooms of quasi-spherical flagellates (e.g. Anglès et al. 2008). However, poor cell abundance estimations are obtained when non-spherical cells dominate the phytoplankton assemblage, because the particle size distribution depends on both the shape of the cell and its relative orientation with respect to the beam of incident light (Gibson et al. 2007). Consequently, we converted the phytoplankton cell abundance estimates from light microscopy and flow cytometry to biovolume. Phytoplankton biovolume was assessed independently for each taxon/species from the cell shape characteristics and geometric models following Olenina et al. (2006).

The rest of the water sample was used for nutrient analysis. Nitrate and nitrite concentrations (NO_3 + NO_2), hereafter dissolved inorganic nitrogen (DIN), were measured with an Alliance autoanalyzer following Grasshoff et al. (1983). Ammonium only represents a small fraction of DIN in these coastal waters and was therefore not measured. The limit of detection, calculated as 3 times the standard deviation of subsequent blank measurements, was 0.001 µM.

Statistical analysis of phytoplankton size distribution

To separate the phytoplankton size distribution from non-algal components, a CCA was applied to the concurrent measurements of particle size distribution from the LISST and pigment concentrations (chl *a*, *b* and *c*) measured by spectrofluorometry from the water samples. Since our LISST-100X measures particles from 2.5 to 500 µm, we completed the lower range of the size spectrum (0.7, 1 and 2.5 µm fractions) using the equivalent volume concentration of the abundances of *Prochlorococcus*, *Synechococcus* and picoeukaryotes, respectively, obtained by flow cytometry, assuming that cells were spherical (Hall & Vincent 1990). These complementary data are not necessary if the more recent version of the instrument (LISST-200X, with size detection of 0.8 to 500 µm) is used.

The CCA seeks basic vectors such that the correlation between the projections of the particle size distribution and pigment concentrations onto these vectors is maximized. In other words, the vectors will correspond to the particle size distributions that are highly related with pigment concentrations. Since non-algal components have no pigments, the resulting vectors for the particle size distribution will be associated with phytoplankton. Different CCA modes will separate the phytoplankton size distribution according to the pigment concentrations, which allows the identification of phytoplankton groups. The mathematical formulation of the CCA is given below and a schematic representation of the procedure is shown in Fig. S2.

We define a particle size matrix X ($n \times m$), containing the particle size distribution from the LISST (complemented with flow cytometry data) for each observation time (n) and for each depth and size bin (m). The length of m is 1295 (35 particle size classes × 37 depth bins). Matrix Y ($n \times k$) contains the pigment concentrations, where k is the number of observations of different pigments. We note that the number of observation times (n) has to be the same for both matrices, but they can have a different number of variables (size bins, number of pigments and sampling depths). Since we measured 3 different pigments (chl *a*, *b* and *c*), the length of k is 15 (3 pigments × 5 depths). The method could be similarly applied to more detailed pigment data (i.e. obtained with HPLC).

The CCA identifies coherent structures between the 2 data matrices X and Y (Hotelling 1936). Briefly, let vector χ be a linear combination of matrix X; that is, vector χ is an ($n \times 1$) vector (temporal evolution of phytoplankton for each mode, in our case) defined by

$$\chi = Xc \tag{1}$$

where c ($m \times 1$) is the base function (phytoplankton size distribution modes) for matrix X. We also defined η ($n \times 1$) (temporal evolution of pigments for each mode) as a linear combination of matrix Y with base function d ($k \times 1$) (pigment modes)

$$\eta = Yd \tag{2}$$

The CCA attempts to find c and d such that the covariance between χ and η is maximum under the conditions where the base functions are orthonormal, $cc' = I$ and $dd' = I$, where I is the identity matrix. The covariance between X and Y is defined as

$$R = \frac{X'Y}{n} \tag{3}$$

Once calculated, the modes are arranged such that the first mode corresponds to the largest eigenvalue, and successively. The percentage of covariance explained by the ith mode, the squared covariance fraction (SCF), is

$$\mathrm{SCF}_i = \frac{(\chi_i \eta_i)^2}{\|R\|^2} \tag{4}$$

where the squared Frobenius matrix norm is the total amount of squared covariance summed over all entries in R. For visualization purposes, the phytoplankton size distribution modes (c vectors) are rearranged in a matrix of 35 particle size classes × 37 depth bins. Similarly, the pigment modes (d vectors) are rearranged in a matrix of 3 pigments × 5 depths.

RESULTS

Abiotic factors

Temperature data show the typical spring to summer transition in Palma Bay, Mallorca, where water column stratification is governed by the seasonal evolution of temperature (Fig. 1a). Minimum temperatures (~15°C) were found in April when the water column was weakly stratified, whereas maximum surface temperatures exceeding 26°C were observed from mid-August to the end of the study period. From late May to September, progressive warming of the surface layer generated a strong thermal gradient at depths of 20 to 30 m. Salinity was mostly uniform during the sampling period (not shown). DIN was typically low (<1 µM) except in the deep layers during April (>2 µM), when the water column was well mixed (Fig. 1b).

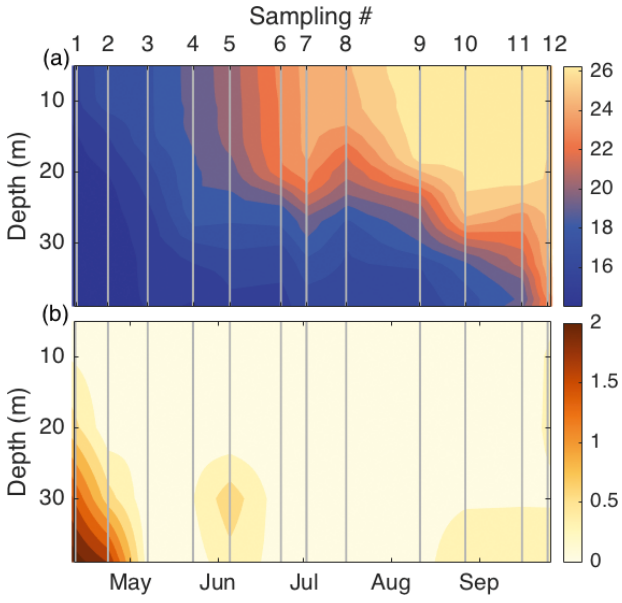

Fig. 1. Evolution of (a) temperature (°C), and (b) dissolved inorganic nitrogen (µM) at Palma Bay during the study period. Vertical grey lines correspond to the sampling dates

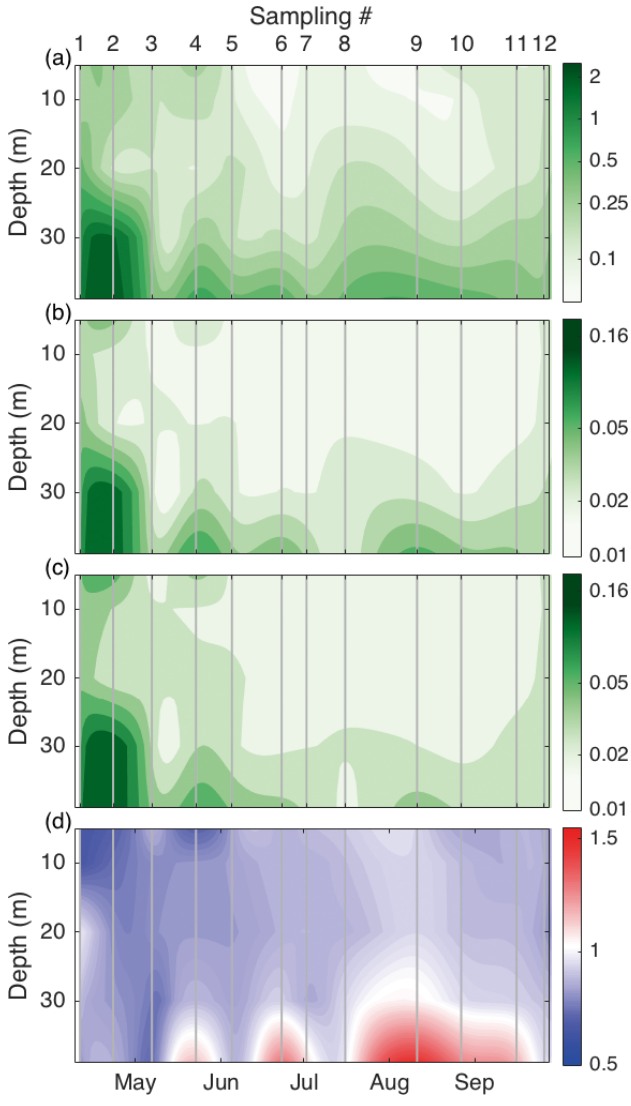

Fig. 2. Evolution of chlorophylls, in mg m^{-3}: (a) chl *a*, (b) chl *b* and (c) chl *c*. (d) Ratio between chl *b* and chl *c*. Vertical grey lines correspond to the sampling dates

Observed phytoplankton dynamics

The evolution of phytoplankton biomass, as determined from chl *a*, is shown in Fig. 2a. The maximum chl *a* concentration was observed during April (sampling 2) at the deep levels (>2.2 mg m^{-3}). The strong thermal gradient likely limited surface phytoplankton biomass during summer (<0.1 mg m^{-3}). Other pigments presented lower concentrations throughout the survey (maximum of 0.2 mg m^{-3}). From these, chl *b* concentration was the highest at deeper levels during summer (Fig. 2b,d, samplings 4, 6–7 and 9–11). In contrast, as indicated by the ratio between chl *b* and chl *c*, chl *c* was comparatively higher at deeper levels during April (samplings 1–3) and near the surface during the entire study period (Fig. 2d). The 3 chl pigments are highly related to DIN and inversely related to temperature, as indicated by a principal component analysis (PCA) of the environmental variables (temperature, salinity, DIN) and pigment data (Fig. S3). This relationship is mainly dictated by the seasonal evolution of temperature and DIN concentration when the thermal gradient intensifies at the beginning of May.

In agreement with the maximum chl *a* concentration, the phytoplankton biovolume was dominated by diatoms such as *Pseudo-nitzschia* sp. and *Chaetoceros* spp., and dinoflagellates such as *Protoperidinium* spp., that peaked during April (sampling 2) at the deep levels (Fig. 3a–c). After this bloom, nanoflagellates became dominant (samplings 3–5) in most of the water column (Fig. 3d). During summer (samplings 8–12), *Prochlorococcus* and pikoeukaryotes were the most abundant species in terms of biovolume, with the latter being restricted to the deeper levels (Fig. 3e,f). The sum of the remaining phytoplankton species only represented a small fraction of the biovolume (Fig. 3h). *Pseudo-nitzschia* sp., *Chaetoceros* spp. and *Protoperidinium* spp. mainly contributed to higher chl *c* at deeper levels during April, while nanoflagellates, *Prochlorococcus*, *Pterosperma* spp. and picoeukaryotes were responsible for chl *b* at deeper levels during summer.

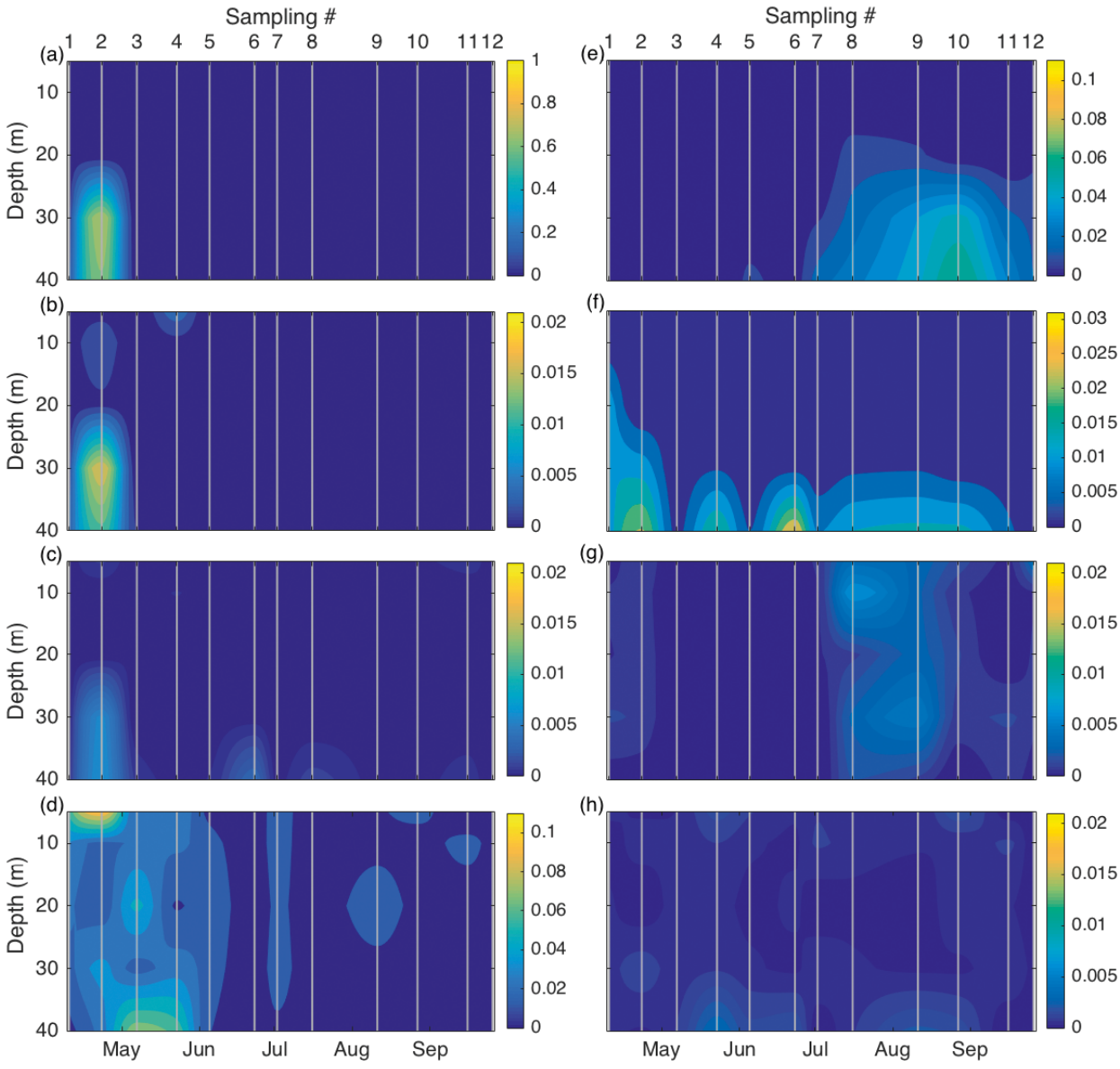

Fig. 3. Evolution of main phytoplankton species or groups, in µl l^{-1}: (a) *Pseudo-nitzschia* sp., (b) *Chaetoceros* spp., (c) *Protoperidinium* spp., (d) nanoflagellates, (e) *Prochlorococcus*, (f) picoeukaryotes, (g) *Pterosperma* spp. and (h) the remaining phytoplankton species. Vertical grey lines correspond to the sampling dates

Observed suspended-particle dynamics

Particle size distribution from the LISST data provides information on the dynamics of suspended particles, which include both phytoplankton and non-algal components. To analyze the main patterns of variation of total suspended particles, we conducted a PCA with particle size distribution data in the size range of 0.7–100 µm. The time-averaged particle size distribution for each depth shows that large particles (20–80 µm) peaked at depths of 30–40 m where mean concentrations exceed 0.04 µl l^{-1}, and also near the surface (50–80 µm; Fig. 4a). A secondary peak of smaller particles (<2 µm) was also found at most depths. The PCA reveals deviations from the time-averaged particle size distribution. The first PCA mode explains 65% of the total particle variance. The corresponding particle size distribution shows positive values for sizes from 0.7 to 100 µm at deeper levels and negative values for sizes from 2.5 to 35 µm at levels above 30 m depth (Fig. 4b). The second PCA mode (Fig. 4c) explains 15% of the variance and rep-

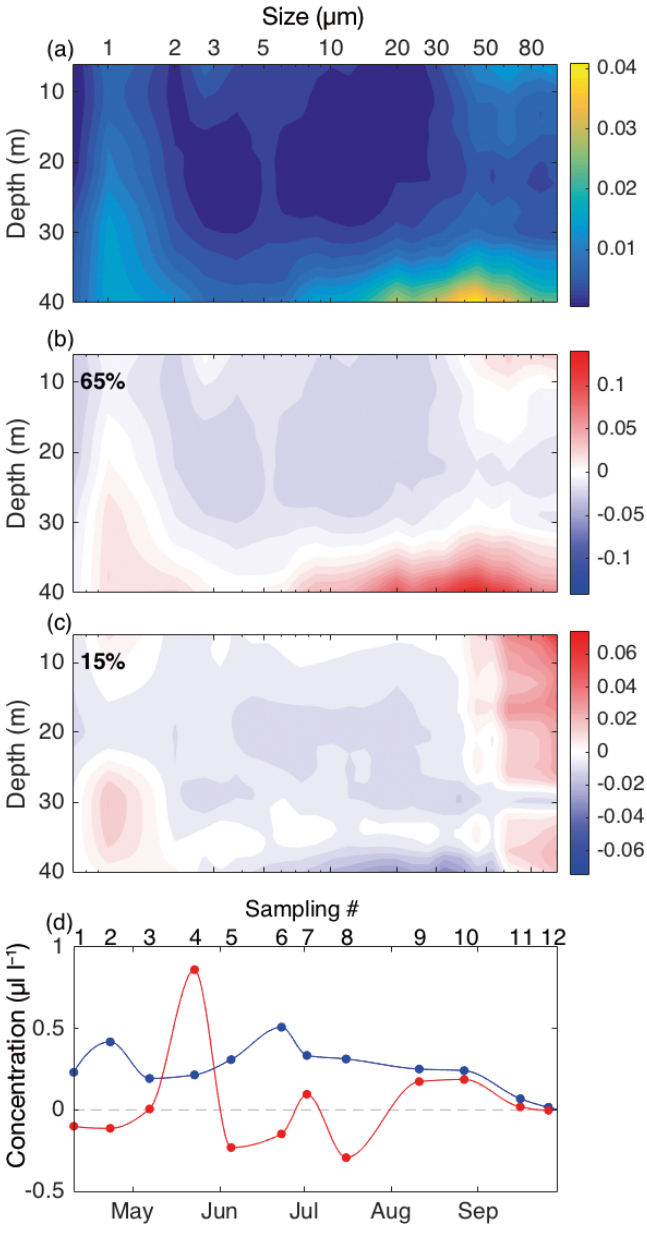

Fig. 4. Total suspended particle size distribution: (a) time averaged volume concentration (µl l^{-1}), (b) first principal component analysis (PCA) mode (which explained 65% of the total particle variance), (c) second PCA mode (which explained 15% of the variance), and (d) temporal variation of the first (blue line) and second (red line) PCA modes. Color bars indicate volume concentrations (µl l^{-1})

resents the variability of very large (>55 µm) and small (<2 µm) particles. Large particles particularly accumulated near the surface, whereas small particles presented a maximum at deeper levels. As shown in Fig. 4d, the temporal variation of the first PCA mode shows positive values from April to September with 2 maxima during samplings 2 and 6. The product of the PCA mode and its temporal evolution indicates the corresponding variation. For example, particles from 0.7 to 100 µm at deeper levels increased from April to September as both (mode and temporal variation) were positive in the first PCA mode. Positive values in the temporal variation of the second PCA mode reveal that very large (>55 µm) particles at the surface and small (<2 µm) particles at deeper levels considerably increased during sampling 4, which took place after 2 d of intense rainfall in the area (>15 mm). The negative peaks with respect to the average during samplings 5, 6 and 8 reveal a decline of these particle sizes.

Estimates of phytoplankton size distribution

As expected, pigment composition and particle size distribution did not compare well. For example, the pigment data displayed in Fig. 2 show high concentrations of chl *c* in April (samplings 1–3) and enhanced chl *b* at deeper levels during summer (samplings 4, 6–7 and 9–10). In contrast, the particle size distribution indicates that particles larger than 7 µm are present at deeper levels (see Fig. 4), especially in samplings 2 and 6, and a remarkable increase of large particles (>55 µm) occurs at the upper levels in May (sampling 4). This reveals an important influence of non-algal particles in the total suspended particles. In addition, the pigment composition agrees fairly well with the biovolume of the dominant species. However, it does not provide information on the involved cell sizes. We used the CCA between pigment composition and particle size distribution to remove the influence of non-algal particles and identify the cell sizes corresponding to the different pigments.

The first CCA mode (Fig. 5), explaining 90% of the combined data variability, reveals a general increase in particle sizes (2–100 µm) and pigments at the deeper levels (30–40 m). The phytoplankton size distribution exhibits peaks at 2.5, 8 and 40 µm, which suggests a community composed of different phytoplankton size groups and/or a dominant phytoplankton species with a non-spherical shape (Fig. 5a). All pigments (chl *a*, *b* and *c*) present a similar contribution to this CCA mode (Fig. 5b–d). The temporal evolution of the CCA mode shown in Fig. 5e indicates that the increase in particles and pigments at deeper levels occurred in April (sampling 2).

The second CCA mode, which explains 8% of the variability, indicates an increase of most particle sizes (peaking at 1, 5, 20 and 60 µm) and pigments (especially chl *b*) at 40 m depth (Fig. 6). This increase

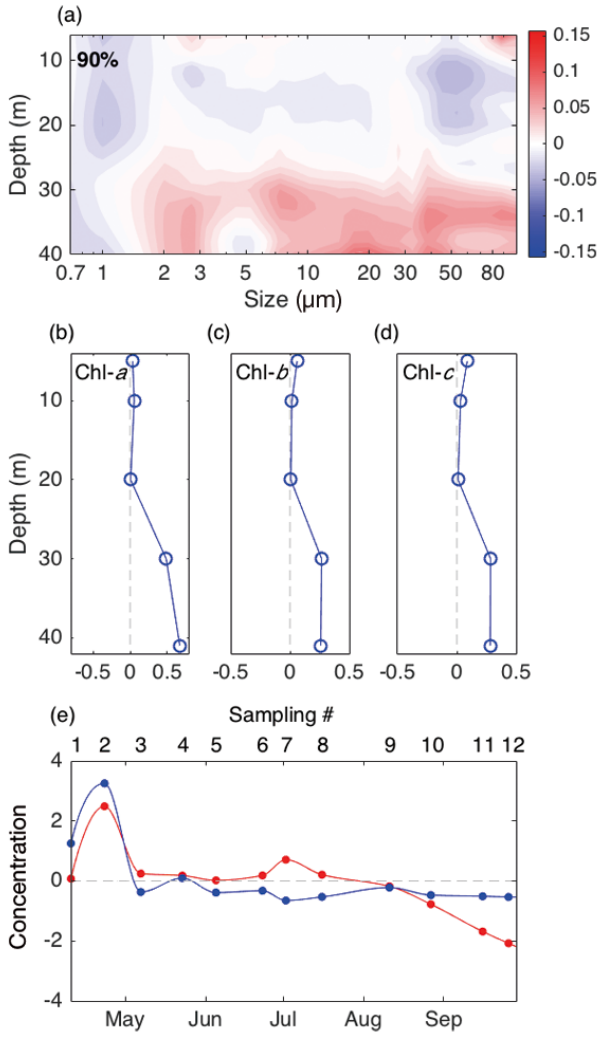

Fig. 5. First canonical correlation analysis (CCA) mode for (a) phytoplankton size distribution (where this mode explained 90% of the combined data variability), (b) chl *a*, (c) chl *b*, (d) chl *c* (all chl in mg m^{-3}) and (e) corresponding temporal variation of phytoplankton size distribution (red line, µl l^{-1}) and chl pigments (blue line, mg m^{-3})

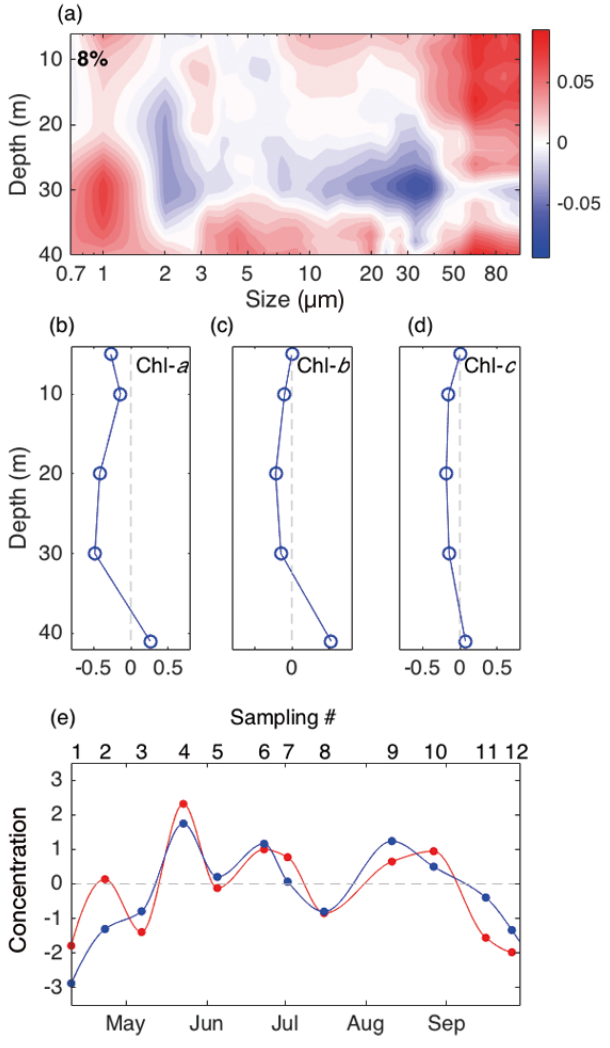

Fig. 6. Second canonical correlation analysis (CCA) mode for (a) phytoplankton size distribution (where this mode explained 8% of the combined data variability), (b) chl *a*, (c) chl *b*, (d) chl *c* (all chl in mg m^{-3}) and (e) corresponding temporal variation of phytoplankton size distribution (red line, µl l^{-1}) and chl pigments (blue line, mg m^{-3})

was accompanied by a reduction of particles smaller than 50 µm and pigments at 30 m. These changes in the water column occurred during summer (samplings 4, 6, 7, 9 and 10). The opposite behavior took place at the beginning and end of the study period (samplings 1–3, 11 and 12) and during sampling 8. Also, an increase of particles larger than 50 µm at levels above 30 m was related to a decrease in pigment concentration.

One of the advantages of the CCA is the removal of the non-algal particle contribution, by identifying coherent structures between particle size distribution and pigment composition. If the contribution of non-algal particles is low, both PCA and CCA components should be highly correlated. The correlations between PCA and CCA components in our case study yield relatively good correlations (0.62 and 0.88 for PCA1/CCA1 and PCA2/CCA2), revealing a low presence of non-algal particles in Palma Bay (Fig. S4). However, the PCA is not able to identify the cell sizes corresponding to the different pigments as the CCA does.

Method validation

Fig. 7 shows the evolution of the total integrated particle size distribution from the LISST measure-

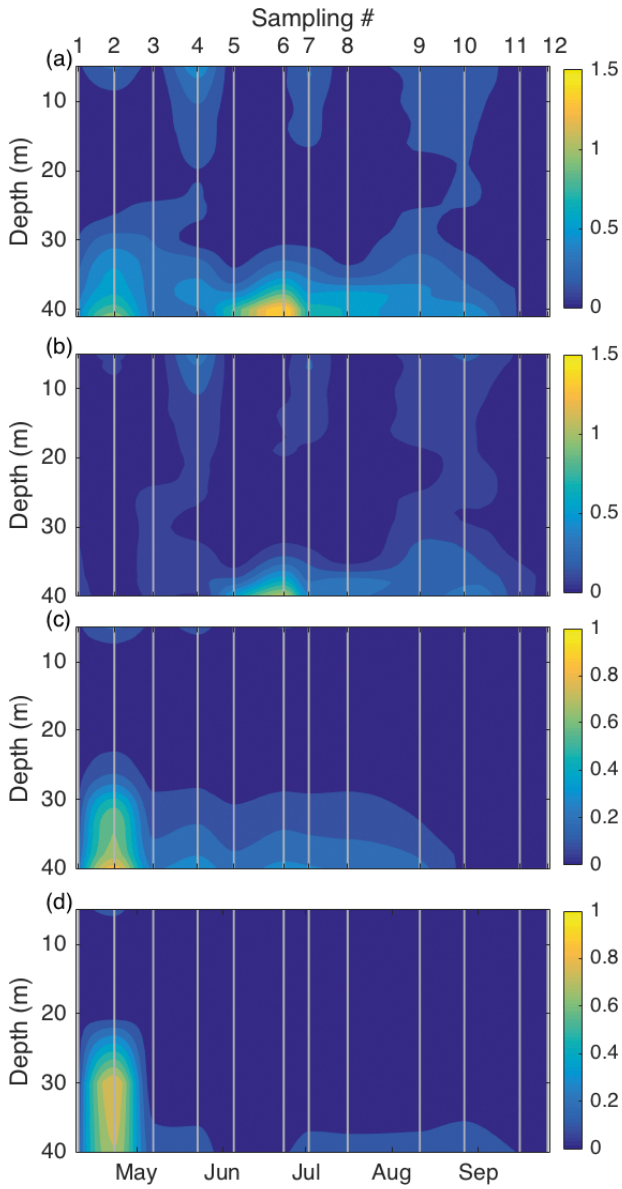

Fig. 7. Evolution (in µl l^{-1}) of the (a) total integrated particle size distribution from the laser *in situ* scattering and transmissometry (LISST) measurements, (b) total integrated non-algal particle size distribution, (c) total integrated phytoplankton size distribution from the canonical correlation analysis, and (d) total phytoplankton biovolume from flow cytometry and microscopy counts. Non-algal particle size distribution was determined from the particle size distribution minus the phytoplankton size distribution

ments, the total integrated non-algal particle size distribution, total integrated phytoplankton size distribution from the CCA and total phytoplankton biovolume (µl l^{-1}) from flow cytometry and microscopy counts. The total integrated particle size distribution was obtained by integrating the LISST data (complemented with flow cytometry) for all size ranges. The total integrated phytoplankton size distribution corresponds to the sum of the first 2 CCA modes for all size ranges. The total integrated non-algal particle size distribution is the total integrated particle size distribution minus the total integrated phytoplankton size distribution. The total phytoplankton biovolume is the biovolume sum of all species and groups determined by flow cytometry and microscopy counts. The comparison between the total integrated particle size distribution and the total phytoplankton biovolume yields a low correlation ($r = 0.35$, $p < 0.01$) due to the influence of non-algal particles. The correlation between the total integrated phytoplankton size distribution and the total phytoplankton biovolume is much better ($r = 0.75$, $p < 0.01$), indicating good performance of the CCA method.

As mentioned before, the CCA is also able to extract information on the cell sizes that correspond to phytoplankton species (or groups) with high content of chl *b* and chl *c*. The results from the CCA indicate that the first mode corresponds to phytoplankton with higher chl *c* and the second mode to higher chl *b* (Figs. 5 & 6). Fig. 8 compares the integrated first 2 modes (sum of all size ranges for each mode) with the dominant species (or groups) from flow cytometry and microscopy counts that contain higher chl *c* (i.e. *Pseudo-nitzschia* sp., *Chaetoceros* spp., *Protoperidinium* spp.) and higher chl *b* (i.e. nanoflagellates, *Prochlorococcus, Pterosperma* spp., picoeukaryotes). Good correlations are obtained between the integrated first CCA mode and the integrated species (or groups) with high chl *c* ($r = 0.72$, $p < 0.01$) and between the integrated second CCA mode and the integrated species (or groups) with high chl *b* ($r = 0.78$ $p < 0.01$).

DISCUSSION

In this study, we proposed and tested a methodology based on the use of CCA in concurrent measurements of particle size distribution and pigment concentrations for analyzing phytoplankton community composition. This method allows separating the algal and non-algal components of the particulate matter while providing information on the different phytoplankton groups. With the constraints of using only 3 pigments (chl *a*, *b* and *c*), we successfully identified the main groups associated with each pigment of the phytoplankton community at a coastal location in the Mediterranean Sea. Indeed, we also obtained valuable quantitative information on phytoplankton biovolume. These biovolume estimations are relevant in

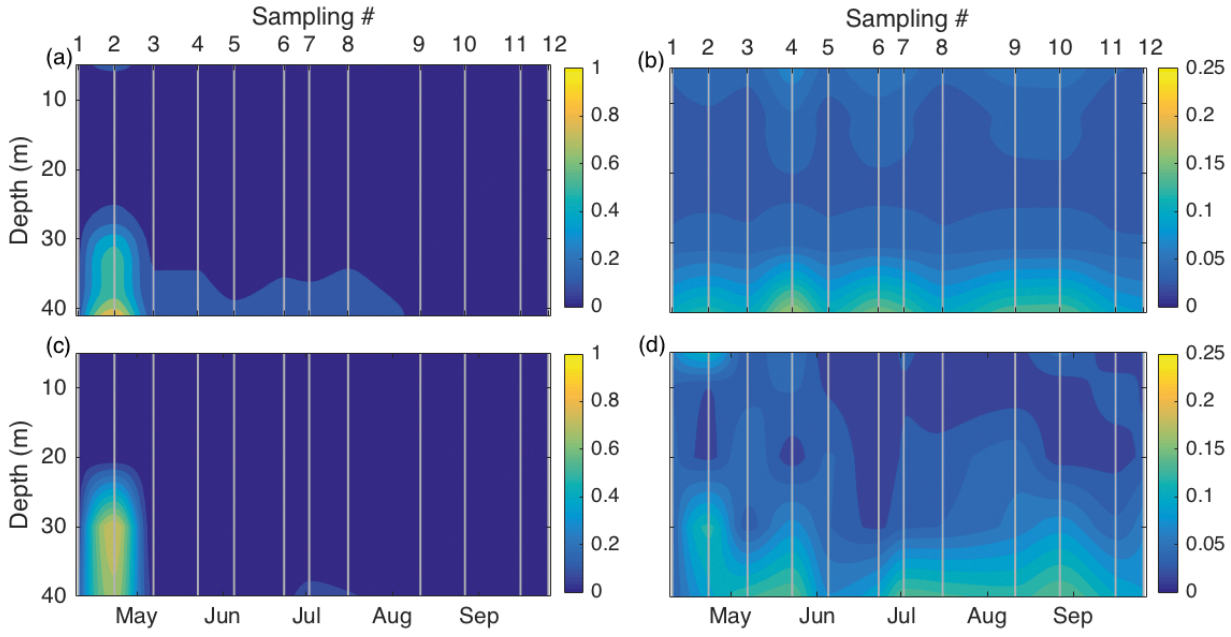

Fig. 8. Evolution (in µl l^{-1}) of the integrated phytoplankton size distribution for (a) the first and (b) the second canonical correlation analysis (CCA) mode, and the integrated phytoplankton biovolume for groups (or species) containing (c) chl *c* and (d) chl *b*

the calculation of algal carbon content that, using other methods, requires many calculations and the use of imprecise conversion factors (e.g. Geider et al. 1997).

Laser transmissometry provides direct measurements of particle size distribution, allowing estimations of phytoplankton size distribution using the proposed CCA. Our results show good agreement when compared to the phytoplankton biovolume derived from flow cytometry and microscopy counts (Fig. 7c,d). A further advantage of the proposed methodology is that information obtained on community size structure may be more regular and more mechanistically interpretable than species composition (Edwards 2016). For example, seasonal variations in temperature and nutrient availability are reflected in complex successional changes in species composition, but interpretation of the structural changes from a large-celled, diatom-dominated community in spring to a small-celled, flagellate-dominated community during the summer may be more straightforward (i.e. Goericke 1998).

While size structure can be assessed by different laboratory techniques, several studies have demonstrated the suitability of LISST to analyze phytoplankton size distribution *in situ* (Serra et al. 2001, Anglès et al. 2008, Barone et al. 2015, Font-Muñoz et al. 2015). For example, Rienecker et al. (2008) showed that peaks in the phytoplankton size distribution can be used to identify the presence of species such as *Pseudo-nitzschia* and *Asterionella* spp. when these species dominate the phytoplankton community. Also, Karp-Boss et al. (2007) demonstrated that the peaks in the size distribution can provide valuable information on the different axes of symmetry of non-spherical cell species like *Ceratium longipes.*

In our case, complementary information on pigment composition helps to overcome the limitations of LISST measurements by using the CCA method. Pigment–size relationships can be used to identify some algal groups or species. Our results show that the spring phytoplankton bloom was characterized by 2 main peaks (8 and 40 µm) and an increase in chl *c*, which suggested diatom dominance. This was corroborated by the microscopy analyses that revealed a high abundance of *Pseudo-nitzschia* sp. This pennate diatom presents a characteristic spectral signature displaying 2 main peaks that correspond to its main axes of symmetry. Likewise, an increase in *Prochlorococcus* was suggested by a peak at sizes <1 µm and a simultaneous increase in chl *b*.

An important aspect of our methodology is the resolution provided by the LISST-100X (1 Hz sampling frequency), especially when compared with the resolution of microscopy counts. High resolution sampling, together with the large volume sample analyzed (~2.5 ml s^{-1}) by the LISST, guarantees better representability of the information provided by this method than by discrete water samples and subsequent microscopy analysis. Further, phytoplankton

size distribution summarizes the structural changes associated with species variations while providing clues on ecosystem level processes such as energy and mass flux (Reul et al. 2006). While acknowledging the importance of detailed identification of phytoplankton species composition in the natural environment, the ecological implications of changes in species composition are often difficult to interpret, particularly when many taxa coexist. This is typically approached by clustering the information associated with different criteria, such as species functionality. For these purposes, size distribution data can be an interesting alternative.

Identification of the spatial and temporal modes of variation achieved by CCA of size and pigment data provides a simplified, yet highly valuable, interpretation of the spatial–temporal variations in phytoplankton structure. This technique only requires particle size and pigment information that may be available from different marine instrumentation and, therefore, can be a good alternative to more sophisticated and costly instrumentation. The limitations of the proposed methodology in the identification of the different phytoplankton groups are mainly imposed by the resolution of the particle size distribution and the number of characteristic pigments analyzed.

Acknowledgements. This study is a result of the MINECO Grant 'GRADIENTS Fine-scale structure of cross-shore GRADIENTS along the Mediterranean coast (CTM2012-39476).' J.S.F.-M.'s work was supported by a PhD fellowship from Conselleria d'Educació (Govern de les Illes Balears) and Fondo Social Europeo (FSE). S.A.'s work was funded by a Marie Skłodowska-Curie International Outgoing Fellowship within the 7th European Community Framework Programme (Project CONPLANK, PIOF-GA-2011-302562). We are grateful to E. Alacid for cytometry analysis and to M. Delgado for microscopy identification of phytoplankton.

LITERATURE CITED

Agrawal YC, Pottsmith HC (2000) Instruments for particle size and settling velocity observations in sediment transport. Mar Geol 168:89–114

Agrawal YC, Whitmire A, Mikkelsen OA, Pottsmith HC (2008) Light scattering by random shaped particles and consequences on measuring suspended sediments by laser diffraction. J Geophys Res 113:C04023

Anglès S, Jordi A, Garcés E, Masó M, Basterretxea G (2008) High-resolution spatio-temporal distribution of a coastal phytoplankton bloom using laser in situ scattering and transmissometry (LISST). Harmful Algae 7:808–816

Anglès S, Jordi A, Campbell L (2015) Responses of the coastal phytoplankton community to tropical cyclones revealed by high-frequency imaging flow cytometry. Limnol Oceanogr 60:1562–1576

Azam F, Fenchel T, Field JG, Gray JS, Meyer-Reil LA, Thingstad F (1983) The ecological role of water-column microbes in the sea. Mar Ecol Prog Ser 10:257–263

Barone B, Bidigare RR, Church MJ, Karl DM, Letelier RM, White AE (2015) Particle distributions and dynamics in the euphotic zone of the North Pacific Subtropical Gyre. J Geophys Res Oceans 120:3229–3247

Beutler M, Wiltshire KH, Meyer B, Moldaenke C and others (2002) A fluorometric method for the differentiation of algal populations *in vivo* and *in situ*. Photosynth Res 72: 39–53

Bornet B, Antoine E, Bardouil M, Baut CML (2004) ISSR as new markers for genetic characterization and evaluation of relationships among phytoplankton. J Appl Phycol 16: 285–290

Boyd PW, Strzepek R, Fu F, Hutchins DA (2010) Environmental control of open-ocean phytoplankton groups: now and in the future. Limnol Oceanogr 55:1353–1376

Campbell L, Henrichs DW, Olson RJ, Sosik HM (2013) Continuous automated imaging-in-flow cytometry for detection and early warning of *Karenia brevis* blooms in the Gulf of Mexico. Environ Sci Pollut Res Int 20:6896–6902

Dugenne M, Thyssen M, Nerini D, Mante C and others (2014) Consequence of a sudden wind event on the dynamics of a coastal phytoplankton community: an insight into specific population growth rates using a single cell high frequency approach. Front Microbiol 5:485

Edwards KF (2016) Community trait structure in phytoplankton: seasonal dynamics from a method for sparse trait data. Ecology 97:3441–3451

Falkowski PG, Raven JA (2013) Aquatic photosynthesis. Princeton University Press, Princeton, NJ

Font-Muñoz JS, Jordi A, Angles S, Basterretxea G (2015) Estimation of phytoplankton size structure in coastal waters using simultaneous laser diffraction and fluorescence measurements. J Plankton Res 37:740–751

Gasol JM, del Giorgio PA (2000) Using flow cytometry for counting natural planktonic bacteria and understanding the structure of planktonic bacterial communities. Sci Mar 64:197–224

Geider RJ, MacIntyre HL, Kana TM (1997) Dynamic model of phytoplankton growth and acclimation: responses of the balanced growth rate and the chlorophyll *a*:carbon ratio to light, nutrient-limitation and temperature. Mar Ecol Prog Ser 148:187–200

Gibb SW, Barlow RG, Cummings DG, Rees NW, Trees CC, Holligan P, Suggett D (2000) Surface phytoplankton pigment distributions in the Atlantic Ocean: an assessment of basin scale variability between 50° N and 50° S. Prog Oceanogr 45:339–368

Gibson RN, Atkinson RJA, Gordon JDM (2007) Inherent optical properties of non-spherical marine-like particles from theory to observation. Oceanogr Mar Biol Annu Rev 45:1–38

Gieskes WWC (1991) Algal pigment fingerprints: clue to taxon-specific abundance, productivity and degradation of phytoplankton in seas and oceans. In: Demers S (ed) Particle analysis in oceanography. NATO ASI series, Springer, Berlin, p 61–99

Gieskes WWC, Kraay GW (1983) Dominance of Cryptophyceae during the phytoplankton spring bloom in the central North Sea detected by HPLC analysis of pigments. Mar Biol 75:179–185

Goericke R (1998) Response of phytoplankton community structure and taxon-specific growth rates to seasonally varying physical forcing in the Sargasso Sea off

Bermuda. Limnol Oceanogr 43:921–935
Goericke R (2011) The size structure of marine phytoplankton — What are the rules? Calif Coop Ocean Fish Invest Rep 52:198–204
Grasshoff K, Ehrhardt M, Kremling K (1983) Methods of seawater analysis. Verlag Chemie, Weinheim
Guinder V, Molinero J (2013) Climate change effects on marine phytoplankton. In: Arias AH, Menendez MC (eds) Marine ecology in a changing world. CRC Press, Boca Raton, FL, p 68–90
Hall JA, Vincent WF (1990) Vertical and horizontal structure in the picoplankton communities of a coastal upwelling system. Mar Biol 106:465–471
Haraguchi L, Jakobsen HH, Lundholm N, Carstensen J (2017) Monitoring natural phytoplankton communities: a comparison between traditional methods and pulse-shape recording flow cytometry. Aquat Microb Ecol 80: 77–92
Harris G (2012) Phytoplankton ecology: structure, function and fluctuation. Springer Science & Business Media, Amsterdam
Hotelling H (1936) Relations between two sets of variates. Biometrika 28:321–377
Huete-Ortega M, Marañón E, Varela M, Bode A (2010) General patterns in the size scaling of phytoplankton abundance in coastal waters during a 10-year time series. J Plankton Res 32:1–14
Irwin AJ, Finkel ZV, Schofield O, Falkowski PG (2006) Scaling-up from nutrient physiology to the size-structure of phytoplankton communities. J Plankton Res 28:459–471
Jakobsen HH, Carstensen J, Harrison PJ, Zingone A (2015) Estimating time series phytoplankton carbon biomass: inter-lab comparison of species identification and comparison of volume-to-carbon scaling ratios. Estuar Coast Shelf Sci 162:143–150
Jeffrey SW, Hallegraeff GM (1987) Chlorophyllase distribution in ten classes of phytoplankton: a problem for chlorophyll analysis. Mar Ecol Prog Ser 35:293–304
Karl DM, Bidigare RR, Letelier RM (2001) Long-term changes in plankton community structure and productivity in the North Pacific Subtropical Gyre: the domain shift hypothesis. Deep-Sea Res II 48:1449–1470
Karp-Boss L, Azevedo L, Boss E (2007) LISST-100 measurements of phytoplankton size distribution: evaluation of the effects of cell shape. Limnol Oceanogr Methods 5: 396–406
Laws EA, Falkowski PG, Smith WO, Ducklow H, McCarthy JJ (2000) Temperature effects on export production in the open ocean. Global Biogeochem Cycles 14:1231–1246
Litchman E, Klausmeier CA (2008) Trait-based community ecology of phytoplankton. Annu Rev Ecol Evol Syst 39: 615–639
Lohrenz SE, Carroll CL, Weidemann AD, Tuel M (2003) Variations in phytoplankton pigments, size structure and community composition related to wind forcing and water mass properties on the North Carolina inner shelf. Cont Shelf Res 23:1447–1464
Mackey MD, Mackey DJ, Higgins HW, Wright SW (1996) CHEMTAX — a program for estimating class abundances from chemical markers: application to HPLC measurements of phytoplankton. Mar Ecol Prog Ser 144: 265–283
Marañón E (2009) Phytoplankton size structure. In: Steele JH, Turekian KK, Thorpe SA (eds) Encyclopedia of ocean sciences. Academic Press, Oxford, p 4252–4256
Marañón E (2015) Cell size as a key determinant of phytoplankton metabolism and community structure. Annu Rev Mar Sci 7:241–264
Margalef R (1963) Succession in marine populations. Adv Front Plant Sci 2:137–188
Marquet PA, Quiñones RA, Abades S, Labra F, Tognelli M, Arim M, Rivadeneira M (2005) Scaling and power-laws in ecological systems. J Exp Biol 208:1749–1769
Millie DF, Paerl HW, Hurley JP (1993) Microalgal pigment assessments using high-performance liquid chromatography: a synopsis of organismal and ecological applications. Can J Fish Aquat Sci 50:2513–2527
Neveux J, Lantoine F (1993) Spectrofluorometric assay of chlorophylls and phaeopigments using the least squares approximation technique. Deep-Sea Res 40: 1747–1765
Neveux J, Panouse M (1987) Spectrofluorometric determination of chlorophylls and pheophytins. Arch Hydrobiol 109: 567–581
Neveux J, Seppälä J, Dandonneau Y (2011) Multivariate analysis of extracted pigments using spectrophotometric and spectrofluorometric methods. In: Roy S, Llewellyn C, Egeland E, Johnsen G (eds) Phytoplankton pigments: characterization, chemotaxonomy and applications in oceanography. Cambridge University Press, New York, NY, p 343–372
Olenina I, Hajdu SEL, Andersson A, Wasmund N and others (2006) Biovolumes and size-classes of phytoplankton in the Baltic Sea. HELCOM Balt Sea Environ Proc No 106. Baltic Marine Environment Protection Commission — Helsinki Commission, Helsinki
Olson RJ, Sosik HM (2007) A submersible imaging-in-flow instrument to analyze nano- and microplankton: Imaging FlowCytobot. Limnol Oceanogr Methods 5:195–203
Ras J, Claustre H, Uitz J (2008) Spatial variability of phytoplankton pigment distributions in the Subtropical South Pacific Ocean: comparison between in situ and predicted data. Biogeosciences 5:353–369
Reul A, Rodríguez J, Blanco JM, Rees A, Burkill PH (2006) Control of microplankton size structure in contrasting water columns of the Celtic Sea. J Plankton Res 28: 449–457
Reynolds RA, Stramski D, Wright VM, Woźniak SB (2010) Measurements and characterization of particle size distributions in coastal waters. J Geophys Res 115:C08024
Rienecker E, Ryan J, Blum M, Dietz C, Coletti L, Marin R, Bissett WP (2008) Mapping phytoplankton in situ using a laser-scattering sensor. Limnol Oceanogr Methods 6: 153–161
Rusch DB, Martiny AC, Dupont CL, Halpern AL, Venter JC (2010) Characterization of *Prochlorococcus* clades from iron-depleted oceanic regions. Proc Natl Acad Sci USA 107:16184–16189
Serra T, Colomer J, Cristina XP, Vila X, Arellano JB, Casamitjana X (2001) Evaluation of laser in situ scattering instrument for measuring concentration of phytoplankton, purple sulfur bacteria, and suspended inorganic sediments in lakes. J Environ Eng 127:1023–1030
Sieracki CK, Sieracki ME, Yentsch CS (1998) An imaging-in-flow system for automated analysis of marine microplankton. Mar Ecol Prog Ser 168:285–296
Sosik HM, Olson RJ (2007) Automated taxonomic classification of phytoplankton sampled with imaging in-flow cytometry. Limnol Oceanogr Methods 5:204–216
Throndsen J (1995) Estimating cell numbers. In: Hallegraeff

GM, Anderson DM, Cembella AD (eds) Manual on harmful marine microalgae. UNESCO, Paris, p 63–80

Thyssen M, Alvain S, Lefèbvre A, Dessailly D and others (2015) High-resolution analysis of a North Sea phytoplankton community structure based on in situ flow cytometry observations and potential implication for remote sensing. Biogeosciences 12:4051–4066

Uitz J, Claustre H, Morel A, Hooker SB (2006) Vertical distribution of phytoplankton communities in open ocean: an assessment based on surface chlorophyll. J Geophys Res 111:C08005

Wright SW, Jeffrey SW, Mantoura RFC (2005) Phytoplankton pigments in oceanography: guidelines to modern methods. UNESCO, Paris

Yentsch CS, Phinney DA (1985) Spectral fluorescence: an ataxonomic tool for studying the structure of phytoplankton populations. J Plankton Res 7:617–632

Zhang F, He J, Su R, Wang X (2011) Assessing phytoplankton using a two-rank database based on excitation-emission fluorescence spectra. Appl Spectrosc 65:1–9

Zingone A, Harrison PJ, Kraberg A, Lehtinen S and others (2015) Increasing the quality, comparability and accessibility of phytoplankton species composition time-series data. Estuar Coast Shelf Sci 162:151–160

Editorial responsibility: Antonio Bode, A Coruña, Spain

Submitted: September 5, 2017; Accepted: March 12, 2018
Proofs received from author(s): April 14, 2018